















Clinical and Preclinical Activity of EGFR Tyrosine Kinase Inhibitors in Non–Small-Cell Lung Cancer Harboring *BRAF* Class 3 Mutations

Alessandro Di Federico, MD^{1,2} ; Stefania Angelicola, MSc^{1,3} ; Mariateresa Frascino, MSc⁴; Irene Siracusa, BSc⁴; Beatrice Bisanti, MSc⁴; Francesca Ruzzi, PhD³ ; Maria Sofia Semprini, MSc³ ; Hugo De Jonge, PhD⁴ ; Andrea De Giglio, MD, PhD^{1,2} ; Francesca Sperandi, MD¹ ; Stefano Brocchi, MD⁵ ; Barbara Melotti, MD¹; Francesca Giunchi, MD⁶ ; Elisa Gruppioni, MS⁷ ; Annalisa Altimari, PhD⁷ ; Pier-Luigi Lollini, PhD^{3,8} ; Andrea Ardizzone, MD^{1,2}; Arianna Palladini, PhD^{4,9} ; and Francesco Gelsomino, MD, PhD^{1,2} 

DOI <https://doi.org/10.1200/PO.24.00240>

ABSTRACT

PURPOSE Patients with tumors harboring *BRAF* class 3 mutations lack targeted therapies. These mutations are characterized by low/absent *BRAF* kinase domain activation and are believed to amplify already active RAS signaling, potentially triggered by receptor tyrosine kinases like EGFR.

MATERIALS AND METHODS Two patients with *BRAF* class 3–mutated metastatic non–small-cell lung cancer (NSCLC) were treated with erlotinib at our Institution after failure of standard therapies. Two cell lines were established from patients with *BRAF* class 3–mutated NSCLC, and their sensitivity to EGFR tyrosine kinase inhibitors (EGFR–TKIs) was assessed using *EGFR*–mutated, *BRAF* class 1 and 2–mutated, and *KRAS*–mutated NSCLC cell lines as controls.

RESULTS Patient 1, a 60-year-old male with *BRAF*^{D594N}–mutated NSCLC, achieved complete response to erlotinib after progression on first- and second-line chemotherapy. Patient 2, a 60-year-old female with *BRAF*^{D594G}–mutated NSCLC, achieved partial response to erlotinib after progression on first-line chemoimmunotherapy. High baseline phosphorylated EGFR values and reduced EGFR activation following erlotinib were observed in *BRAF* class 3–mutated and *EGFR*–mutated cell lines, but not in *BRAF* class 1–mutated, *BRAF* class 2–mutated, or *KRAS*–mutated lines. Erlotinib inhibited 2-dimensional growth in *BRAF* class 3–mutated cell lines (IC₅₀ 6.33 and 7.11 μM) and in the *BRAF* class 2–mutated cell line (IC₅₀ 5.51 μM), albeit at higher concentrations than in *EGFR*–mutated lines, whereas it showed no effect on *BRAF* class 1–mutated (IC₅₀, >25 μM) or *KRAS*–mutated (IC₅₀, >25 μM) lines. These findings were corroborated by 3-dimensional and sphere formation assays. In the Cancer Cell Line Encyclopedia, *BRAF* class 3–mutated NSCLC cell lines showed greater sensitivity to EGFR–TKIs compared with *BRAF* class 2–mutated and *KRAS*–mutated lines.

CONCLUSION *BRAF* class 3 mutations in NSCLC may identify a novel targetable population sensitive to EGFR–TKIs.

ACCOMPANYING CONTENT

 Appendix

 Data Supplement

Accepted October 22, 2024

Published December 5, 2024

JCO Precis Oncol 8:e2400240

© 2024 by American Society of
Clinical Oncology

INTRODUCTION

BRAF alterations occur in approximately 2%–5% of non-squamous non–small-cell lung cancer (NSCLC) and can be classified into three functional classes on the basis of their effect on the *BRAF* kinase domain.^{1,2} Class 1, represented by *BRAF*^{V600} mutations, strongly activates the *BRAF* kinase domain as a monomer, driving the constitutive activation of the downstream MAPK pathway independently of RAS activation. Class 2 alterations are characterized by

intermediate-to-high activity of the *BRAF* kinase domain, acting as *BRAF* dimers and maintaining independence from RAS for the downstream signaling process. Class 3 mutations exhibit low-to-absent activation of the *BRAF* kinase domain but enhance affinity with RAS, forming heterodimers with CRAF and amplifying a pre-existing RAS signal, which results in the activation of downstream pathways.² Although *BRAF* and MEK inhibitors are effective for patients with NSCLC harboring *BRAF*^{V600} mutations, no targeted therapies have demonstrated convincing clinical activity for patients

CONTEXT

Key Objective

To assess the activity of the EGFR tyrosine kinase inhibitor (EGFR-TKI) erlotinib in *BRAF* class 3–mutated non–small-cell lung cancer (NSCLC).

Knowledge Generated

We report for the first time the clinical activity of the EGFR-TKI erlotinib in two patients with metastatic *BRAF* class 3–mutated NSCLC and further validated this by establishing two patient-derived cell lines sensitive to EGFR-TKIs. Erlotinib and osimertinib effectively inhibited the growth of *BRAF* class 3–mutated cell lines while showing limited to no effect on *BRAF* class 1–mutated or *KRAS*-mutated lines.

Relevance

BRAF class 3 mutations may identify patients with NSCLC who could benefit from existing targeted therapies, paving the way for clinical trials in a population currently orphan of targeted treatments.

with *BRAF*^{non-V600} alterations, particularly class 3 mutations.^{3–5} In NSCLC harboring *BRAF* class 3 mutations, RAS activation by receptor tyrosine kinases like EGFR has been observed, suggesting mutant *BRAF* amplifies EGFR-triggered RAS signaling.⁶ Although three generations of EGFR tyrosine kinase inhibitors (EGFR-TKIs) are proven to be effective for patients with NSCLC with *EGFR* mutations, their potential against *BRAF* class 3 mutations remains unexplored.⁷ This study sought to provide the rationale and preliminary evidence of the activity of EGFR-TKIs for patients with *BRAF* class 3–mutated NSCLC.

MATERIALS AND METHODS

Patient Identification

We searched for patients with advanced or metastatic NSCLC harboring *BRAF* class 3 mutations without other concurring driver alterations detected by next-generation sequencing (NGS) panel (OncoPrint Focus Assay; ThermoFisher Scientific, Kit RUO, Milan, Italy) who were treated with EGFR-TKIs in our institution, identifying two patients treated with erlotinib 150 mg once daily after failure of standard treatments, as per its approval based on the BR.21 study.⁸ Clinicopathologic, genomic, and outcomes data of these patients were collected by a medical oncologist (A.D.F.) through manual chart review.

The study was conducted in accordance with the Declaration of Helsinki. Human samples were collected after patients gave their informed consent. The protocol was approved by the institutional review board and by the Ethics Committee Center Emilia–Romagna Region, Italy (GR-2018-12368031). Human samples and metadata including relevant clinical data were deidentified before being shared between laboratories involved in this study. All animal procedures were performed in accordance with European directive 2010/63/UE and Italian Law (No. DL26/2014); experimental protocols

were reviewed and approved by the institutional animal care and use committee of the University of Bologna and by the Italian Ministry of Health with letter 32/2020-PR.

Establishment of Cell Lines and Patient-Derived Xenograft Models

A patient-derived xenograft (PDX) was established from a lymph node metastasis of one of the two patients with *BRAF* class 3–mutated NSCLC treated with erlotinib, harboring a *BRAF*^{D594G} mutation, before the administration of the EGFR-TKI, through the implantation of a tumor biopsy fragment in a BALB/c Rag2^{-/-}; Il2rg^{-/-} (BRG) immunodeficient mouse.⁹ PDX-ADK-36 cell culture was derived from the tumor mass grown after the second in vivo passage. In parallel, a second cell line was established from a biopsy of a lymph node metastasis of a patient with stage IV NSCLC and a *BRAF*^{G466V} class 3 mutation at progression to first-line pembrolizumab (ADK-14), and a third cell line from a patient with untreated NSCLC harboring a *KRAS*^{G12V} mutation to serve as a control (ADK-17). The ADK-14 cell line was established and cultured in MammoCult (STEMCELL Technologies, Vancouver, Canada) supplemented with 1% fetal bovine serum (FBS; Thermo Fisher Scientific). PDX-ADK-36 and ADK-17 cell lines were established and cultured in Roswell Park Memorial Institute (RPMI) medium (Thermo Fisher Scientific) supplemented with 10% FBS. In addition, two *EGFR*-mutated (PC-9 and HCC-827, both with an E746_A750del mutation) pre-established NSCLC cell lines, one *BRAF* class 1–mutated pre-established NSCLC cell line (HCC-364, with a V600E mutation), and one *BRAF* class 2–mutated NSCLC pre-established cell line (NCI-H1395, with a G469A mutation) were used as controls. PC-9 and HCC-827 were cultured in RPMI + 10% FBS. HCC-364 and NCI-H1395 were cultured in Dulbecco's Modified Eagle Medium (DMEM) + 10% FBS; 100 U/mL penicillin and 10 μg/mL streptomycin (Thermo Fisher Scientific) were added to all mediums, and cells were grown at 37°C in a humidified atmosphere at 5% CO₂.

Drug Sensitivity in 2-Dimensional Culture Condition

Cells were seeded at 5,000 cells/well into a 96-well plate in MammoCult + 1% FBS (ADK-14), RPMI + 10% FBS (HCC-827, PDX-ADK-36 and ADK-17), or DMEM + 10% FBS (HCC-364, NCI-H1395). PC-9 cells were seeded at 1,000 cells/well into a 96-well plate in RPMI + 10% FBS. After 24 hours from seeding, cells were treated with drugs (all by Selleck Chemicals, Houston, TX) by adding 10 μ L of a 10 \times solution of each drug or vehicle (for TKIs: DMSO, Merck, Milan, Italy; for cetuximab: only cell culture medium) in each well. Cell growth was assessed 72 hours later by the WST-1 cell proliferation assay (Merck) according to the manufacturer's instructions.

Drug Sensitivity in 3-Dimensional Culture Condition

ADK-14 and PDX-ADK-36 cells were seeded at 500 cells/well in a 24-well plate in semisolid medium—MammoCult + 1% FBS + 0.33% agar (Sea-Plaque Agarose, Lonza, Switzerland), containing drugs, with a 0.5% agarose underlay. HCC-364 and NCI-H1395 were seeded at 4,000 cells/well in a 24-well plate in semisolid medium—DMEM + 10% FBS + 0.33% agar, containing drugs, with a 0.5% agarose underlay. HCC-827 and ADK-17 cells were seeded at 2,000 cells/well and PC-9 at 500 cells/well in a 24-well plate in semisolid medium—RPMI + 10% FBS + 0.33% agar, containing drugs, with a 0.5% agarose underlay. Colonies (diameter, >90 μ m) were counted 2–4 weeks later under an inverted microscope in dark field, as previously described.¹⁰

Sphere Formation Assay

Cells were seeded at 10,000 cells (5,000 cells for NCI-H1395) in 4 mL complete MammoCult medium without serum in 6-well Ultra-Low adherence plate (Corning Life Sciences, Corning, NY), according to the MammoCult Human Medium Kit protocol. Drugs and vehicle were added to the medium at different doses. Cells were incubated at 37°C in a humidified 5% CO₂ atmosphere for a week. Spheres, multicell structures with a diameter larger than 90 μ m, were counted about 7 days after the seeding.¹⁰

Western Blotting

Protein extraction, quantification, and Western blotting were performed as previously reported.¹⁰ The effect of drugs was evaluated by exposing cells to the treatment for 6 hours. Treatment was added the day after seeding. An untreated and a vehicle-treated sample ran in parallel as controls. Anti-EGFR monoclonal antibody (clone D38B1, diluted 1:1,000), anti-phospho-EGFR (Tyr1068) monoclonal antibody (clone D7A5, diluted 1:500), anti-ERK1/2 monoclonal antibody (clone 137F5, diluted 1:1,000), and anti-phospho-ERK1/2 (Thr202/Tyr204) monoclonal antibody clone (clone D13.14.4E, diluted 1:500) were used as primary antibodies. Mouse monoclonal anti-actin antibody (clone 8H10D10, 1:3,000) or anti-vinculin antibody (clone V284, 1:2,000) was used to detect reference proteins. Anti-vinculin antibody

was purchased by Merck, and all the other primary antibodies were purchased from Cell Signaling Technology (Danvers, MA). Membranes were incubated with polyclonal horseradish peroxidase-conjugated anti-rabbit and anti-mouse Immunoglobulin G antibodies (Bio-Rad Laboratories, Milan, Italy). Re-Blot Plus Strong Solution (Merck) was used if needed. Proteins were detected by chemiluminescent reactions visualized using the digital imaging system Azure C600 (Azure Biosystems, Dublin, CA). Protein abundance was defined through densitometric analysis of bands by Azure Spot software (Azure Biosystems).

Statistical Analysis

Comparisons with continuous variables were computed using the Mann-Whitney *U* test, the *t* test, or the Kruskal-Wallis test, as appropriate. All *P* values are two-sided, and confidence intervals are at the 95% level, with significance predefined to be at *P* < .05. Statistical analyses were performed using Prism GraphPad version 10 and R version 3.6.3. half maximal inhibitory concentration (IC₅₀) was calculated using Prism GraphPad version 10 for the following analyses: inhibitor versus normalized response for erlotinib and osimertinib in 2-dimensional assays; inhibitor versus normalized response-variable slope for cetuximab for all cell lines except HCC-827, for which the value was calculated using the absolute IC₅₀ analysis; inhibitor versus normalized response-variable slope for erlotinib in 3-dimensional (3D) and spheres. Inhibition of EGFR phosphorylation by erlotinib was performed by one-sample *t* test, and the mean of each analyzed group was compared with the hypothetical mean of 100. The number of replicates is reported in figure legends.

RESULTS

Antitumor Activity of Erlotinib in Two Patients With BRAF Class 3–Mutated NSCLC

Two patients with stage IV lung adenocarcinoma harboring a BRAF class 3 mutation without other concurrent genomic driver alterations were treated with erlotinib after standard treatments. Patient 1, a 60-year-old male, former smoker, was diagnosed with stage IVB lung adenocarcinoma for lymph node and brain metastases in 2010. A first-line treatment with chemotherapy (carboplatin AUC5 day 1 plus gemcitabine 1,000 mg/m² days 1, 8 every 3 weeks) was administered for four cycles, and stereotactic radiation therapy was effectively performed on the single brain metastasis. Following intrathoracic nodal progressive disease (PD) at the first radiographic tumor reassessment after chemotherapy initiation, a second-line treatment with docetaxel (75 mg/m² every 3 weeks) was administered for a total of 10 cycles, obtaining stable disease as best response. Disease progression was subsequently evidenced on a mediastinal lymph node, for which a third-line treatment with erlotinib 150 mg once daily was initiated in July 2011, leading to a complete response (Fig 1). NGS performed on tissue collected before the initiation of erlotinib documented a BRAF^{D594N} class 3 mutation and a

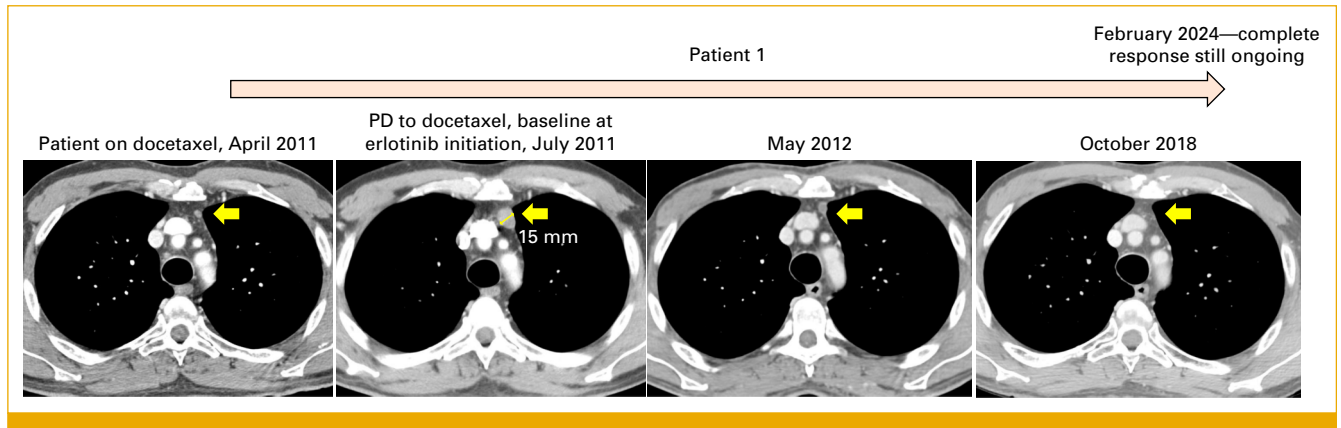


FIG 1. Radiographic assessment of erlotinib activity in patient 1. Computed tomography scans of patient 1 showing the tumor response to erlotinib after PD to docetaxel, with documented gradual shrinkage of a prevascular lymph node metastasis over time. PD, progressive disease.

CTNNB1^{S37C} mutation. The patient is still receiving erlotinib with persistent complete response after 12 years.

Patient 2, a 60-year-old female, heavy smoker, was diagnosed in 2021 with stage IVB lung adenocarcinoma for pleural, bone, and lymph node metastases (Fig 2). NGS showed a BRAF^{D594G} class 3 mutation. PD-L1 tumor proportion score was 0% (clone SP263, Ventana, Roche Diagnostics, Milan, Italy). First-line chemoimmunotherapy (carboplatin AUC5, pemetrexed 500 mg/m², and pembrolizumab 200 mg every 3 weeks) was administered for three cycles before clinical and radiographic evidence of PD. Given the evidence of primary treatment resistance and considering our experience with patient 1, a second-line treatment with erlotinib 150 mg once daily was started. After 1 month of treatment, computed tomography scans showed an objective partial response, with a decrease of 40% or more in measurable tumor lesions (Fig 2). Unfortunately, the patient died few days after tumor reassessment at home, likely due to an acute cardiovascular event, although the exact cause of death could not be documented.

Activity of Erlotinib in BRAF Class 3–Mutated NSCLC Cell Lines

To further investigate on our clinical findings, we derived cell lines from patient 2 (PDX-ADK-36) and from another patient with NSCLC carrying a BRAF^{G466V} class 3 mutation (ADK-14). Two EGFR-mutated cell lines (HCC-827 and PC-9, both with the EGFR^{E746_A750del}), one BRAF class 1–mutated cell line (HCC-364, with a BRAF^{V600E}), one BRAF class 2–mutated cell line (NCI-H1395, with a BRAF^{G469A}), and one KRAS-mutated cell line (ADK-17, with a KRAS^{G12V}) were used as controls. Hypothesizing an overactivation of wild-type EGFR in BRAF class 3–mutated NSCLC cells, Western blots were performed in the seven cell lines. After 30 hours of seeding, we observed high levels of phosphorylated EGFR (pEGFR) in the two BRAF class 3–mutated cell lines (PDX-ADK-36 and ADK-14) and in the two EGFR-mutated cell lines

(HCC-827 and PC-9), but not in the KRAS-mutated (ADK-17), BRAF class 1–mutated (HCC-364), and BRAF class 2–mutated (NCI-H1395) cell lines (Fig 3A). Consistent with our hypothesis, the first-generation EGFR-TKI erlotinib significantly reduced EGFR activation, expressed as pEGFR/EGFR ratio, in the two BRAF class 3–mutated cell lines (PDX-ADK-36 and ADK-14) and in the two EGFR-mutated (HCC-827 and PC-9) cell lines compared with the vehicle ($P < .05$), but not in the KRAS- (ADK-17), BRAF class 1– (HCC-364), and BRAF class 2–mutated (NCI-H1395) cell lines (Fig 3B). Notably, erlotinib did not affect the levels of phosphorylation of ERK in the two BRAF class 3–mutated cell lines (PDX-ADK-36 and ADK-14; Appendix Fig A1). Next, the in vitro activity of erlotinib was evaluated. Erlotinib inhibited the growth of the two BRAF class 3–mutated cell lines: PDX-ADK-36 (IC₅₀, 6.33 μM; SE, 2.13) and ADK-14 (IC₅₀, 7.11 μM; SE, 0.73; Fig 3C; Appendix Table A1). As expected, the growth of the two EGFR-mutated cell lines was also inhibited at lower doses (HCC-827: IC₅₀, 0.06 μM; SE, 0.005; PC-9: IC₅₀, 0.04 μM; SE, 0.004), whereas no effect on the growth of the BRAF class 1–mutated cell line (HCC-364: IC₅₀, >25 μM) and the KRAS-mutated cell line (ADK-17: IC₅₀, >25) was observed (Fig 3C; Appendix Table A1). Notably, the growth of the BRAF class 2–mutated cell line was also inhibited at doses similar to those inhibiting BRAF class 3–mutated cell lines (NCI-H1395: IC₅₀, 5.51 μM; SE, 1.60; Fig 3C; Appendix Table A1), consistent with previous findings on the direct inhibiting effect of EGFR-TKIs on the BRAF^{G469}-mutated protein.¹¹ Since 3D models may allow a better interpretation of TKI activity, erlotinib was tested also on 3D soft agar cultures and sphere formation assays.¹² Consistent with previous observations, erlotinib reduced the 3D soft agar growth of the two BRAF class 3–mutated cell lines, PDX-ADK-36 (IC₅₀, 0.23 μM; SE, 0.04) and ADK-14 (IC₅₀, 1.01 μM; SE, 0.22), as well as that of the two EGFR-mutated cell lines (HCC-827: IC₅₀, <0.01 μM; PC-9: IC₅₀, 0.03 μM; SE, 0.02) and the BRAF class 2–mutated cell line (NCI-H1395: IC₅₀, 0.05 μM; SE, 0.02). Instead, on comparison, erlotinib had a dismal effect on the growth of the BRAF class 1–mutated cell line (HCC-

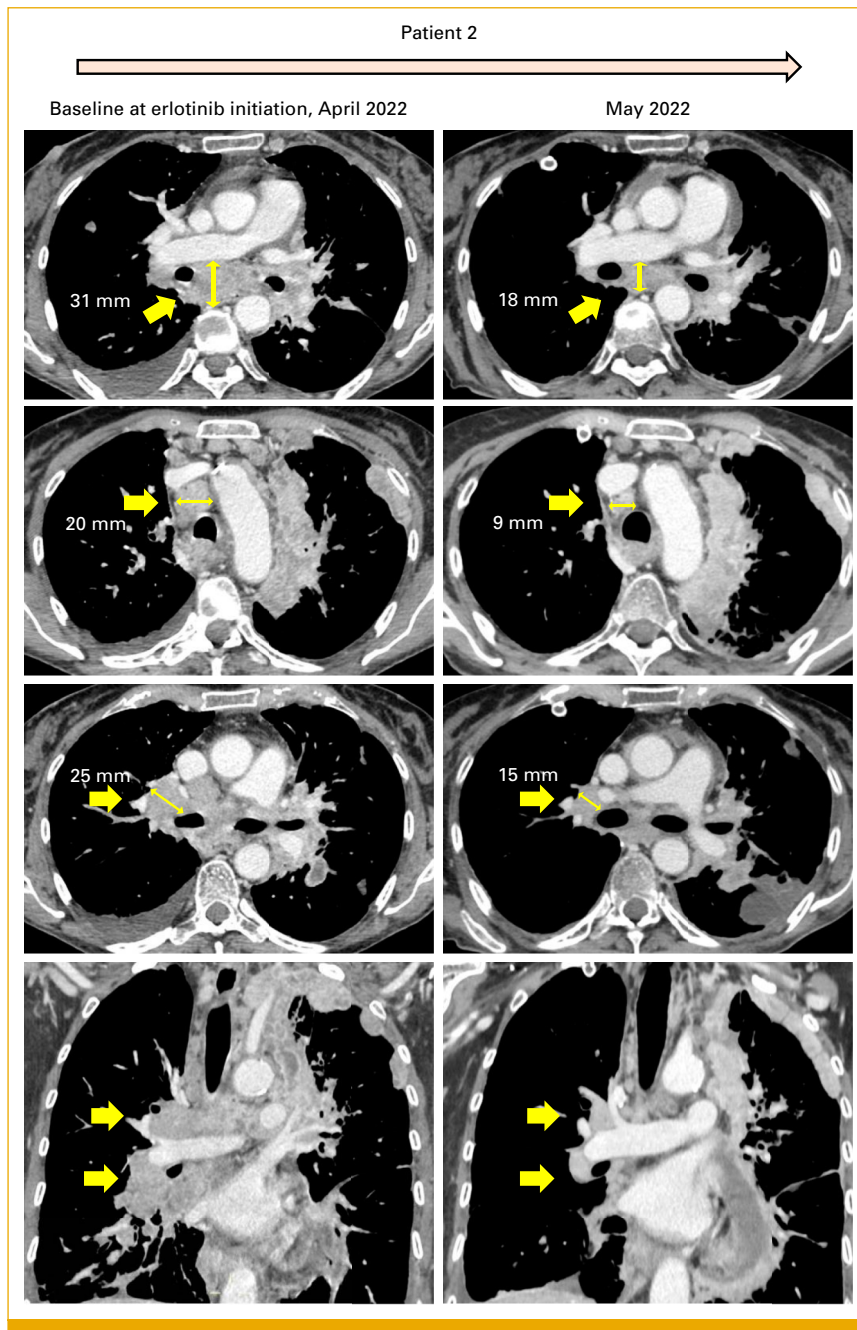


FIG 2. Radiographic assessment of erlotinib activity in patient 2. Computed tomography scans showing the tumor response to erlotinib in patient 2, with documented shrinkage of measurable disease in right hilar, subcarinal, and right upper paratracheal lymph node metastases.

364: IC_{50} , 5.81 μ M; SE, 0.12) and the *KRAS*-mutated cell line (ADK-17: IC_{50} , >10; Fig 3D). Similar findings were observed with sphere formation assays, as erlotinib exerted the strongest effect on *EGFR*-mutated cells (HCC-827: IC_{50} , <0.01 μ M; PC-9: IC_{50} , 0.05 μ M; SE, 0.01), followed by *BRAF* class 3–mutated cells (PDX-ADK-36: IC_{50} , 0.11 μ M; SE, 0.02; ADK-14: IC_{50} , 0.34 μ M; SE, 0.04) and *BRAF* class 2–mutated cells (NCI-H1395: IC_{50} , 4.75 μ M; SE, 1.63), whereas a remarkably weaker effect was observed in *BRAF* class 1–

(HCC-364: IC_{50} , 12.67 μ M; SE, 0.86) and *KRAS*-mutated cells (ADK-17: IC_{50} , 9.34 μ M; SE, 0.46; Fig 3E).

Activity of Other *EGFR*-Directed and Non-*EGFR*-Directed Agents in *BRAF* Class 3–Mutated NSCLC Cell Lines

Following our observations, we explored whether the sensitivity of *BRAF* class 3–mutated NSCLC cell lines was limited

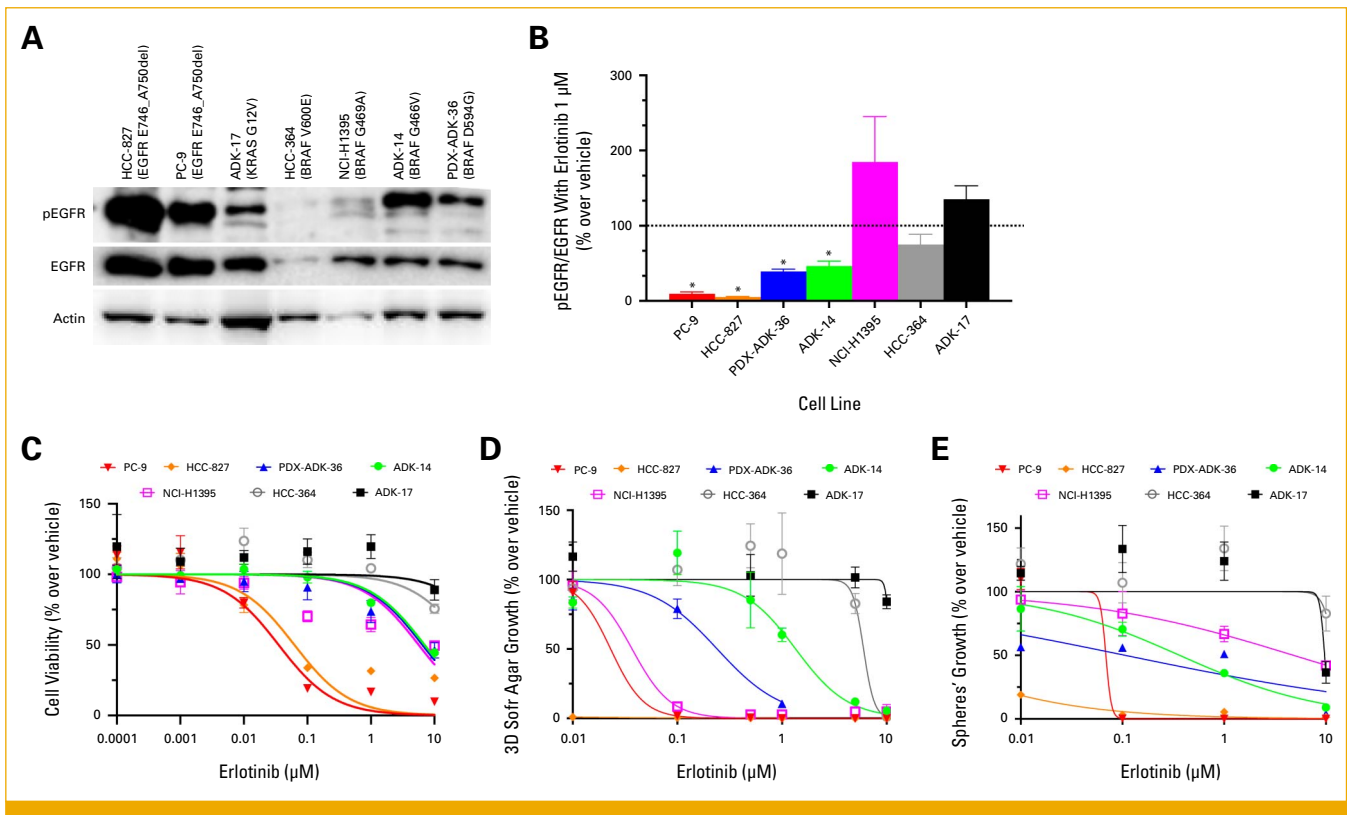


FIG 3. Baseline EGFR activation and comparative sensitivity of cell lines to erlotinib. (A) Western blots showing baseline EGFR activation, evaluated 30 hours after seeding. (B) Effect of erlotinib administration on EGFR phosphorylation, measured as pEGFR/EGFR ratio ($n = 2-4$ replicates). (C) Effect of progressively increasing doses of erlotinib ($n = 2-5$ experiments, each one with three replicates) on cell 2D growth. (D) Effect of progressively increasing doses of erlotinib ($n = 2-4$ replicates) on 3D cell growth in soft agar. (E) Effect of progressively increasing doses of erlotinib ($n = 2-4$ replicates) on sphere formation capability. * $P < .05$ over vehicle. 2D, 2-dimensional; 3D, 3-dimensional; PDX, patient-derived xenograft; pEGFR, phosphorylated EGFR.

to the first-generation EGFR-TKI or could be extended to osimertinib, a third-generation EGFR-TKI currently representing the standard of care for patients with EGFR-mutated NSCLCs. We observed that osimertinib inhibited the growth of the two BRAF class 3-mutated cell lines (PDX-ADK-36: IC₅₀, 1.61 μM ; SE, 0.32; ADK-14: IC₅₀, 7.17 μM ; SE, 2.20), although at higher doses compared with the two EGFR-mutated cell lines (HCC-827: IC₅₀, 0.009 μM ; SE, 0.003; PC-9: IC₅₀, 0.04 μM ; SE, 0.02; Appendix Fig A2A). Again, an inhibitory effect was also observed on the BRAF class 2-mutated cell line (NCI-H1395: IC₅₀, 1.63 μM ; SE, 0.58), whereas no effect was observed on the BRAF class 1-mutated cell line (HCC-364: IC₅₀, >18 μM) or on the KRAS-mutated cell lines (ADK-17: IC₅₀, >149 μM ; Appendix Fig A2A). Sensitivities to the EGFR-directed monoclonal antibody cetuximab are shown in Appendix Figure A2B.

To provide an external validation for our findings, we interrogated the Cancer Cell Line Encyclopedia (Broad, 2019) via cBioPortal¹³⁻¹⁶ for NSCLC cell lines harboring BRAF class 3 mutations. Two cell lines of BRAF class 3-mutated NSCLC and available treatment data were identified, both with the BRAF^{G466V} class 3 mutation, which is identical to the mutation found in ADK-14, and without other concurrent driver

alteration. In addition, cell lines of NSCLC harboring BRAF class 2 ($N = 5$), EGFR ($N = 5$), and KRAS ($N = 36$) mutations were identified and used as controls (Data Supplement). All included driver mutations were classified as oncogenic or likely oncogenic by OncoKB.¹⁷ EGFR mutations only included exon 19 deletions or L858R mutations, and cell lines harboring an EGFR T790M co-mutation were excluded given their known lack of sensitivity to first- and second-generation EGFR-TKIs. We explored the sensitivity of these cell lines to multiple agents, including EGFR-TKIs of first (gefitinib) and second generation (afatinib), a MEK inhibitor (trametinib), a BRAF inhibitor (dabrafenib), a multi-TKI (cabozantinib), and chemotherapy (doxorubicin; Data Supplement). Statistically significant differences in drug sensitivity among the four oncogene-addicted cell lines were only observed when exposed to the EGFR-TKIs gefitinib ($P = .02$) and afatinib ($P = .02$), mainly driven by their higher activity in BRAF class 3-mutated and EGFR-mutated cell lines compared with BRAF class 2-mutated and KRAS-mutated cell lines (Fig 4). Specifically, BRAF class 3-mutated cell lines exhibited a median IC₅₀ of 0.51 μM (range, 0.26-0.77) when treated with gefitinib and 0.52 μM (range, 0.06-0.97) when treated with afatinib. These values were significantly lower than the median IC₅₀ observed among

BRAF class 2–mutated (gefitinib: 6.9 μM , $P = .03$; afatinib: 8.06 μM , $P = .008$) and *KRAS*–mutated cell lines (gefitinib: 5.17 μM , $P = .04$; afatinib: 4.21 μM , $P = .06$), but comparable with the IC_{50} displayed by *EGFR*–mutated cell lines (gefitinib: 0.23 μM , $P = .67$; afatinib: 0.11 μM , $P = .52$; Figs 4A and 4B). No differences in sensitivity to other agents were observed across cell lines (Figs 4C–4F).

DISCUSSION

Patients with NSCLC harboring *BRAF*^{non-V600} alterations are a heterogeneous population in terms of clinicopathologic characteristics, genomic landscape, and BRAF kinase domain activity.¹⁸ These patients are currently orphans of targeted therapies and are treated as nononcogene–addicted, representing a relevant unmet clinical need. In this study, we demonstrate that *BRAF* class 3–mutated NSCLC may be targeted by EGFR–TKIs. Similar to the National Cancer Institute exceptional response initiative, our study started from a clinical retrospective observation: two patients with

EGFR wild-type NSCLC who responded to erlotinib.¹⁹ Then, we established *BRAF* class 3–mutated NSCLC cell lines and confirmed their sensitivity to EGFR–TKIs. We further validated our findings using an independent, publicly available data set. In our experiments, a *BRAF* class 2–mutated cell line harboring the *BRAF*^{G469A} mutation used as one of the controls exhibited sensitivity to EGFR–TKIs, comparable with that observed in *BRAF* class 3–mutated cell lines. However, it did not show high levels of EGFR activation or a reduced pEGFR/EGFR ratio following erlotinib treatment. These observations align with those of a recent study indicating that NSCLC harboring a *BRAF*^{G469V} class 2 mutation may respond to EGFR–TKIs via direct binding to the mutant BRAF protein.¹¹ However, this mechanism appears unlikely to apply to *BRAF* class 3 mutations, given the absence of intrinsic BRAF kinase activity characterizing them, the elevated EGFR activation found in cells harboring these mutations, and its reduction under erlotinib treatment.⁵ Therefore, we hypothesize that in *BRAF* class 3–mutated NSCLC, the mutant BRAF protein amplifies a RAS signal already triggered upstream by a hyperactivated

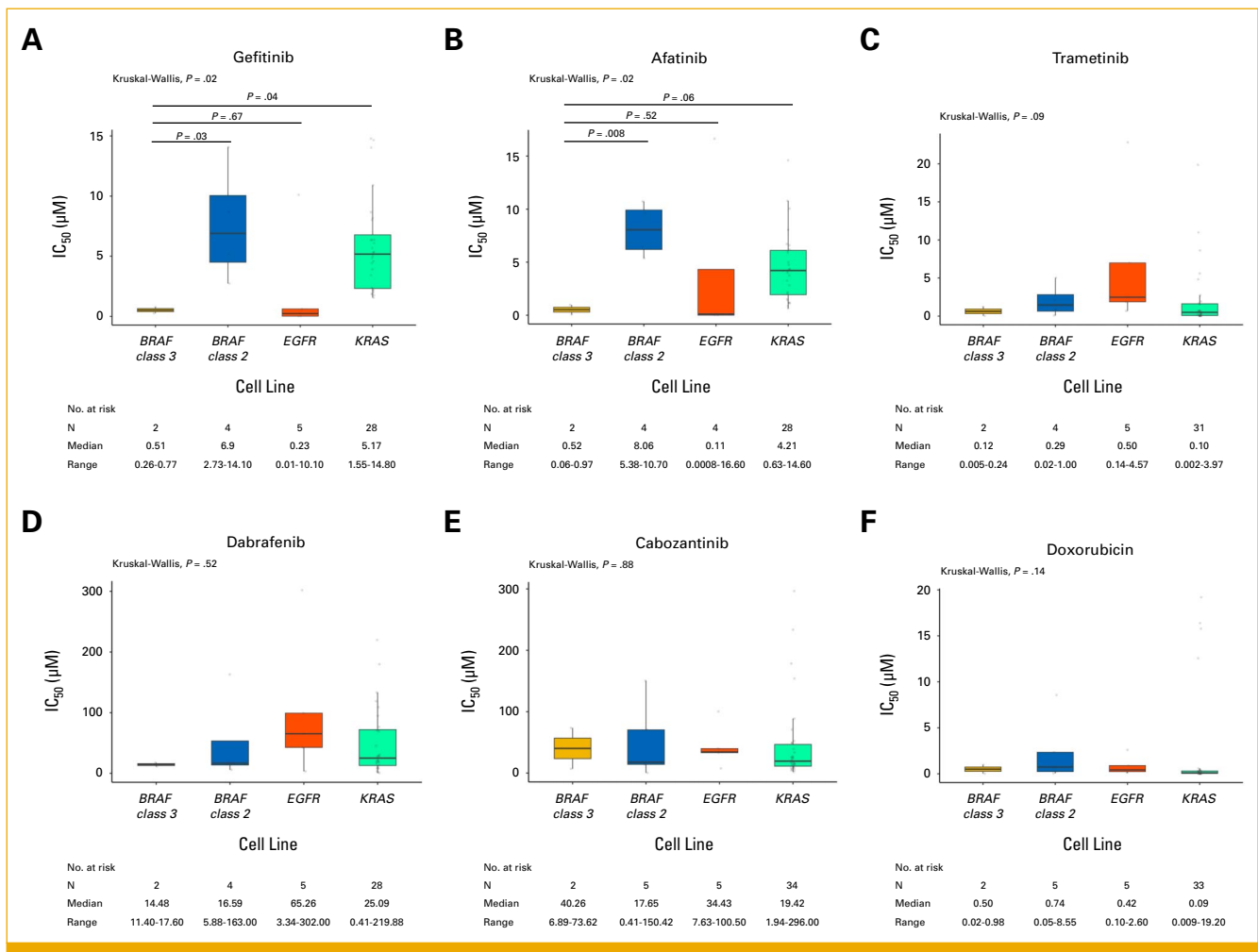


FIG 4. Activity of multiple agents in non–small-cell lung cancer cell lines with *BRAF* class 3, *BRAF* class 2, *EGFR*, or *KRAS* driver alterations in the Cell Line Encyclopedia. Activity, expressed as median IC_{50} , of the EGFR inhibitors (A) gefitinib and (B) afatinib, (C) the MEK inhibitor trametinib, (D) the BRAF inhibitor dabrafenib, (E) the multityrosine kinase inhibitor cabozantinib, and (F) doxorubicin. IC, half maximal inhibitory concentration.

wild-type EGFR, a signal insufficient on its own to drive cancer proliferation without the *BRAF* mutation. Hyperphosphorylation of the EGFR receptor has been previously reported in *BRAF* class 3–mutated NSCLC and colorectal cancer (CRC) cells, but not in malignant melanoma cells.⁶ Consistently, EGFR inhibition with erlotinib or cetuximab was effective in *BRAF* class 3–mutated NSCLC and CRC cell lines. Moreover, anti-EGFR antibodies have demonstrated high activity in patients with metastatic *BRAF* class 3–mutated CRC while showing low activity in those harboring class 2 mutations.^{6,20} Notably, other potential targets reported to be active in some cases of *BRAF* class 3–mutated tumors, such as MET, and erlotinib off-target effects that may contribute to cell growth inhibition were not explored in this study and may be object of further investigation in future research.⁶

To our knowledge, this is the first report of the clinical activity of EGFR inhibition in patients with *BRAF* class 3–

mutated NSCLC. The main limitation of this study is the availability of only two patients treated with erlotinib, reflecting the low prevalence of *BRAF* class 3 mutations in NSCLC (approximately 1%) and the historically limited use of erlotinib in later lines of treatment for *EGFR* wild-type patients. Nevertheless, the strengths of this study include the consistency between clinical and preclinical data and the reproducibility of our findings in an independent data set.

In conclusion, the activation of wild-type EGFR may play a significant role in *BRAF* class 3–mutated NSCLC, which currently represents a population orphan of targeted therapies, suggesting that these tumors might be responsive to EGFR-TKIs. These findings warrant validation through prospective clinical studies, as *BRAF* class 3 mutations might identify an additional subset of patients with NSCLC who could benefit from existing targeted therapies.

AFFILIATIONS

¹Medical Oncology, IRCCS Azienda Ospedaliero-Universitaria di Bologna, Bologna, Italy

²Department of Medical and Surgical Sciences (DIMEC), University of Bologna, Bologna, Italy

³Laboratory of Immunology and Biology of Metastasis, Department of Medical and Surgical Sciences (DIMEC), University of Bologna, Bologna, Italy

⁴Department of Molecular Medicine, University of Pavia, Pavia, Italy

⁵Department of Radiology, IRCCS Azienda Ospedaliero-Universitaria di Bologna, Bologna, Italy

⁶Pathology Unit, IRCCS Azienda Ospedaliero-Universitaria di Bologna, Bologna, Italy

⁷Solid Tumor Molecular Pathology Laboratory, IRCCS Azienda Ospedaliero-Universitaria di Bologna, Bologna, Italy

⁸IRCCS Azienda Ospedaliero-Universitaria di Bologna, Bologna, Italy

⁹Unità Operativa di Oncologia, Fondazione IRCCS Policlinico San Matteo, Pavia, Italy

CORRESPONDING AUTHOR

Arianna Palladini, PhD; e-mail: arianna.palladini@unipv.it.

EQUAL CONTRIBUTION

A.D.F. and S.A. co-first authors. A.P. and F.G. co-last authors.

SUPPORT

Supported by Ricerca Finalizzata Ministero della Salute 2018 grant, number GR-2018-12368031 (to F. Gelsomino, F. Giunchi, A. Palladini).

AUTHOR CONTRIBUTIONS

Conception and design: Alessandro Di Federico, Andrea De Giglio, Francesca Sperandi, Stefano Brocchi, Barbara Melotti, Francesca Giunchi, Andrea Ardizzoni, Francesco Gelsomino

Financial support: Francesco Gelsomino

Administrative support: Francesco Gelsomino

Provision of study materials or patients: Alessandro Di Federico, Stefania Angelicola, Francesca Sperandi, Francesca Giunchi, Arianna Palladini, Francesco Gelsomino

Collection and assembly of data: Alessandro Di Federico, Stefania Angelicola, Mariateresa Frascino, Irene Siracusa, Beatrice Bisanti, Francesca Ruzzi, Maria Sofia Semprini, Barbara Melotti, Francesca Giunchi, Arianna Palladini, Francesco Gelsomino

Data analysis and interpretation: Alessandro Di Federico, Hugo De Jonge, Barbara Melotti, Elisa Gruppioni, Annalisa Altimari, Pier-Luigi Lollini, Andrea Ardizzoni, Arianna Palladini, Francesco Gelsomino

Manuscript writing: All authors

Final approval of manuscript: All authors

Accountable for all aspects of the work: All authors

AUTHORS' DISCLOSURES OF POTENTIAL CONFLICTS OF INTEREST

The following represents disclosure information provided by authors of this manuscript. All relationships are considered compensated unless otherwise noted. Relationships are self-held unless noted. I = Immediate Family Member, Inst = My Institution. Relationships may not relate to the subject matter of this manuscript. For more information about ASCO's conflict of interest policy, please refer to www.asco.org/rwc or ascopubs.org/po/author-center.

Open Payments is a public database containing information reported by companies about payments made to US-licensed physicians ([Open Payments](http://OpenPayments)).

Alessandro Di Federico

Honoraria: Society for Immunotherapy of Cancer

Consulting or Advisory Role: Novartis, Hanson Wade

Hugo De Jonge

Research Funding: Boehringer Ingelheim

Patents, Royalties, Other Intellectual Property: I am inventor on the following patent related to molecules for regenerative medicine. WO2016116577A1 with the title: Met receptor agonist proteins

Andrea De Giglio

Travel, Accommodations, Expenses: Daiichi Sankyo Europe GmbH

Pier-Luigi Lollini

Research Funding: Expres2ion Biotechnologies

Andreas Ardizzoni

Consulting or Advisory Role: BMS, Merck, Roche, AstraZeneca, Lilly

Research Funding: Celgene (Inst), BMS (Inst), Ipsen (Inst), Roche (Inst)

Francesco Gelsomino

Consulting or Advisory Role: Novartis, BMS, Eli-Lilly, AstraZeneca, Regeneron, Pfizer

No other potential conflicts of interest were reported.

ACKNOWLEDGMENT

EGFR-mutated PC-9 and HCC-827 lung cancer cell lines were kindly provided by Prof. Roberta Alfieri and Andrea Cavazzoni from the University of Parma, Parma, Italy. *BRAF*-mutated HCC-364 and NCI-H1395 lung cancer cell lines were kindly provided by Dr. David Santamaria from the Centro de Investigación del Cáncer, Salamanca, Spain.

REFERENCES

- Lamberti G, Andrini E, Sisi M, et al: Beyond EGFR, ALK and ROS1: Current evidence and future perspectives on newly targetable oncogenic drivers in lung adenocarcinoma. *Crit Rev Oncol Hematol* 156:103119, 2020
- Dankner M, Rose AAN, Rajkumar S, et al: Classifying *BRAF* alterations in cancer: New rational therapeutic strategies for actionable mutations. *Oncogene* 37:3183-3199, 2018
- Planchard D, Besse B, Groen HJM, et al: Phase 2 study of dabrafenib plus trametinib in patients with *BRAF* V600E-mutant metastatic NSCLC: Updated 5-year survival rates and genomic analysis. *J Thorac Oncol* 17:103-115, 2022
- Nebhan CA, Johnson DB, Sullivan RJ, et al: Efficacy and safety of trametinib in non-V600 *BRAF* mutant melanoma: A phase II study. *Oncologist* 26:731-e1498, 2021
- Dankner M, Lajoie M, Moldoveanu D, et al: Dual MAPK inhibition is an effective therapeutic strategy for a subset of class II *BRAF* mutant melanomas. *Clin Cancer Res* 24:6483-6494, 2018
- Yao Z, Yaeger R, Rodrik-Outmezguine VS, et al: Tumours with class 3 *BRAF* mutants are sensitive to the inhibition of activated RAS. *Nature* 548:234-238, 2017
- Johnson M, Garassino MC, Mok T, et al: Treatment strategies and outcomes for patients with *EGFR*-mutant non-small cell lung cancer resistant to *EGFR* tyrosine kinase inhibitors: Focus on novel therapies. *Lung Cancer* 170:41-51, 2022
- Shepherd FA, Rodrigues Pereira J, Ciuleanu T, et al: Erlotinib in previously treated non-small-cell lung cancer. *N Engl J Med* 353:123-132, 2005
- Nomura T, Tamaoki N, Takakura A, et al: Basic concept of development and practical application of animal models for human diseases. *Curr Top Microbiol Immunol* 324:1-24, 2008
- Ruzzi F, Angelicola S, Landuzzi L, et al: ADK-VR2, a cell line derived from a treatment-naïve patient with *SDC4-ROS1* fusion-positive primarily crizotinib-resistant NSCLC: A novel preclinical model for new drug development of *ROS1*-rearranged NSCLC. *Transl Lung Cancer Res* 11:2216-2229, 2022
- Huo KG, Notsuda H, Fang Z, et al: Lung cancer driven by *BRAF*G469V mutation is targetable by *EGFR* kinase inhibitors. *J Thorac Oncol* 17:277-288, 2022
- De Giovanni C, Nicoletti G, Quagliano E, et al: Vaccines against human *HER2* prevent mammary carcinoma in mice transgenic for human *HER2*. *Breast Cancer Res* 16:R10, 2014
- de Bruijn I, Kundra R, Mastrogiacomo B, et al: Analysis and visualization of longitudinal genomic and clinical data from the AACR Project GENIE Biopharma Collaborative in cBioPortal. *Cancer Res* 83:3861-3867, 2023
- Cerami E, Gao J, Dogrusoz U, et al: The cBio cancer genomics portal: An open platform for exploring multidimensional cancer genomics data. *Cancer Discov* 2:401-404, 2012 [Erratum: *Cancer Discov* 2:960, 2012]
- Gao J, Aksoy BA, Dogrusoz U, et al: Integrative analysis of complex cancer genomics and clinical profiles using the cBioPortal. *Sci Signal* 6:p11, 2013
- Ghandi M, Huang FW, Jané-Valbuena J, et al: Next-generation characterization of the Cancer Cell Line Encyclopedia. *Nature* 569:503-508, 2019
- Chakravarty D, Gao J, Phillips SM, et al: OncoKB: A precision oncology knowledge base. *JCO Precis Oncol* 10.1200/PO.17.00011
- Di Federico A, De Giglio A, Gelsomino F, et al: Genomic landscape, clinical features and outcomes of non-small cell lung cancer patients harboring *BRAF* alterations of distinct functional classes. *Cancers (Basel)* 14:3472, 2022
- Conley BA, Staudt L, Takebe N, et al: The exceptional responders initiative: Feasibility of a National Cancer Institute pilot study. *J Natl Cancer Inst* 113:27-37, 2021
- Yaeger R, Kotani D, Mondaca S, et al: Response to anti-*EGFR* therapy in patients with *BRAF* non-V600-mutant metastatic colorectal cancer. *Clin Cancer Res* 25:7089-7097, 2019

APPENDIX

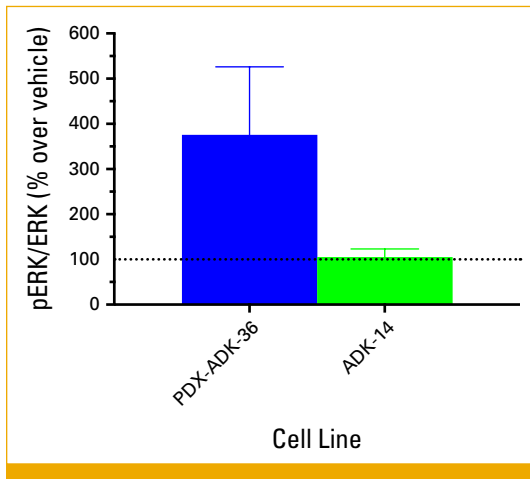


FIG A1. Effect of erlotinib on ERK phosphorylation in *BRAF* class 3–mutated cell lines. Effect of erlotinib treatment (1 μ M) for 6 hours on ERK phosphorylation in PDX-ADK-36 and ADK-14, measured as pERK/ERK ratio. PDX, patient-derived xenograft; pEGFR, phosphorylated EGFR.

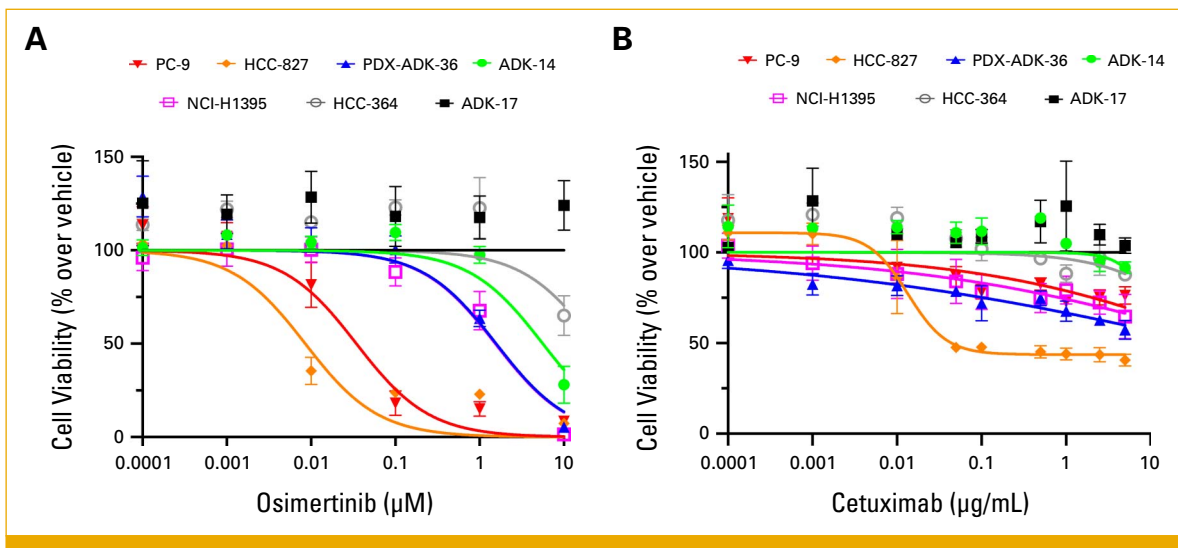


FIG A2. Comparative sensitivities to osimertinib and cetuximab. Effect of progressively increasing doses of (A) osimertinib (n = 2-6 experiments, each one with three replicates) and (B) cetuximab (n = 2-3 experiments, each one with three replicates) on cell 2D growth. 2D, 2-dimensional.

TABLE A1. IC₅₀ (μM) Values for Each Experiment in Cell Lines Tested for Erlotinib 2D Growth Inhibition

Experiment Number	Cell Line						
	PC-9	HCC-827	PDX-ADK-36	ADK-14	NCI-H1395	HCC-364	ADK17
1	0.04099	0.06233	9.232	5.597	3.903	25.56	8.15E + 40
2	0.02704	0.05408	10.07	6.183	7.108	31.93	1.28E + 33
3	0.03751	0.07072	5.207	8.695	—	48.88	25.84
4	—	—	0.806	7.963	—	—	81.84
5	—	—	—	—	—	—	34.83

Abbreviations: 2D, 2-dimensional; IC, half maximal inhibitory concentration; PDX, patient-derived xenograft.